JACS
JOURNAL OF THE AMERICAN CHEMICAL SOCIETY

ARTICLE

pubs.acs.org/JACS

Prioritization of Charge over Geometry in Transition State Analogues of a Dual Specificity Protein Kinase

Liu Xiaoxia,[†,‡] James P. Marston,[†] Nicola J. Baxter,[†,§] Andrea M. Hounslow,[†] Zhao Yufen,[‡] G. Michael Blackburn,[†] Matthew J. Cliff,[*,†] and Jonathan P. Waltho[*,†,§]

[†]Krebs Institute and Department of Molecular Biology & Biotechnology, University of Sheffield, Sheffield S10 2TN, United Kingdom

[‡]Fujian Key Laboratory for Chemical Biology, College of Chemistry and Chemical Engineering, Xiamen University, 361005 Fujian Province, People's Republic of China

[§]Manchester Interdisciplinary Biocentre, University of Manchester, Manchester M1 7DN, United Kingdom

Supporting Information

ABSTRACT: The direct observation of a transition state analogue (TSA) complex for tyrosine phosphorylation by a signaling kinase has been achieved using ^{19}F NMR analysis of MEK6 in complex with tetrafluoroaluminate (AlF_4^-), ADP, and p38α MAP kinase (acceptor residue: Tyr182). Solvent-induced isotope shifts and chemical shifts for the AlF_4^- moiety indicate that two fluorine atoms are coordinated by the two catalytic magnesium ions of the kinase active site, while the two remaining fluorides are liganded by protein residues only. An equivalent, yet distinct, AlF_4^- complex involving the alternative acceptor residue in p38α (Thr180) is only observed when the Tyr182 is mutated to phenylalanine. The formation of octahedral AlF_4^- species for both acceptor residues, rather than the trigonal bipyramidal AlF_3^0 previously identified in the only other metal fluoride complex with a protein kinase, shows the requirement of MEK6 for a TSA that is isoelectronic with the migrating phosphoryl group. This requirement has hitherto only been demonstrated for proteins having a single catalytic magnesium ion.

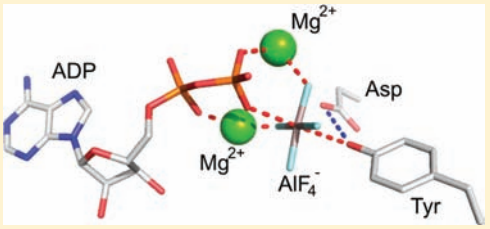

INTRODUCTION

Catalysis of phosphoryl transfer reactions involves some of the largest enzymatic rate accelerations in biology, with uncatalyzed phosphate monoester hydrolysis[1a] at physiological pH and temperature having an extraordinarily long half-life of 10^{20} s. This kinetic stability is all the more remarkable in the light of the fundamental dynamic roles of phosphate esters in biology.[2] Phosphoryl transfer is generally understood to occur through in-line approach of the attacking group and departure of the leaving group at the anionic phosphoryl moiety (Figure 1A).[3] The reaction proceeds through a transition state (TS) species of trigonal bipyramidal geometry, in which the migrating phosphorus atom is surrounded by three equatorial oxygens located in a trigonal plane.

A substantial step forward in understanding the fundamental mechanism of phosphoryl group transfer by enzymes has come about through the use of aluminum[4] and magnesium[5] fluoride species and vanadium and tungsten oxyanions[6] as transition state analogues (TSAs) of the planar phosphoryl, PO_3^-, group. The metal fluoride TSA complexes are particularly informative because ^{19}F NMR can be used to validate the chemical interpretation of X-ray diffraction data and to report on the local electrostatic and protonic environments in the vicinity of the transferring phosphoryl group.[7−11] In the Protein Data Bank, there are presently over 80 high-resolution structures of TSA complexes containing metal fluorides. Recent work has demonstrated that trigonal bipyramidal (TBP) trifluoromagnesate (MgF_3^-) complexes readily assemble in the active site of a range of phosphoryl transfer enzymes,[5,7,8,11,12] where the MgF_3^- moiety is axially coordinated by donor and acceptor oxygen atoms. MgF_3^- is isoelectronic and close to isosteric with the transferring PO_3^- group. By contrast, TSA complexes involving tetrafluoroaluminate (AlF_4^-) have four fluorides in a square planar arrangement around the octahedral Al^{3+} ion with axial coordination by the donor and acceptor groups (Figure 1B). They also are isoelectronic TSAs but necessarily are nonisosteric because of their octahedral structure. However, because of the greater solution stability of the AlF_4^- anion at neutral pH relative to MgF_3^-, aluminum outcompetes magnesium for enzyme metal fluoride complex formation by a factor of at least 500-fold for phosphoryl transfer enzymes studied to date.[8] This indicates that these enzymes are prioritizing retention of anionic charge rather than geometry[8] in their choice of a surrogate for PO_3^-.

Detailed analysis of the TSA complexes establishes that the number of positively and negatively charged groups in the vicinity of the active site is exactly balanced only when it is occupied by a monoanionic species, such as MgF_3^- or AlF_4^-.[11] Such analysis has been applied to a growing number of enzymes to endorse the concept of "charge balance" as a general feature of transition state structures of phosphoryl transfer enzymes.[2] This concept has gained independent validation from the observation

Received: October 6, 2010
Published: February 24, 2011

dx.doi.org/10.1021/ja1090035 | J. Am. Chem. Soc. 2011, 133, 3989–3994

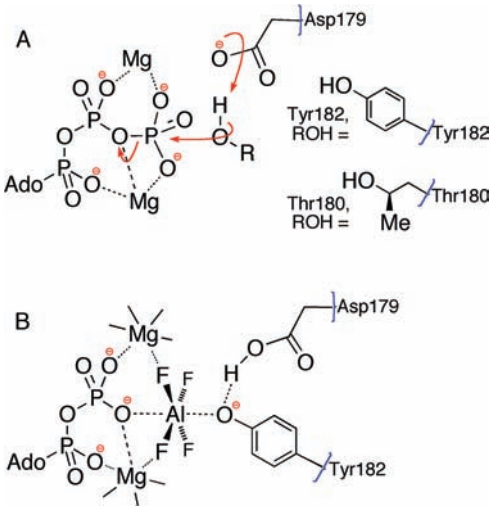

Figure 1. (A) Schematic of the phosphoryl transfer reaction catalyzed by MEK6. (B) Schematic of the proposed AlF_4^--based TSA for the reaction in (A).

that human phosphoglycerate kinase (PGK) responds to mutation as it predicts: the deletion of one positively charged residue from the active site of PGK by the mutation K219A induces a corresponding reduction in the negative charge of the bound aluminum fluoride species; viz., tetrafluoroaluminate (AlF_4^-) is replaced by trifluoroaluminate (AlF_3^0).[11] Hitherto, the dominance of charge balance in TS organization of phosphoryl transfer enzymes has been established only for enzymes containing a single catalytic Mg^{2+} ion.[11] However, numerous phosphoryl transfer enzymes possess two catalytic Mg^{2+} ions, including the superfamily of protein kinases.[13]

Protein kinases comprise 518 genes in the human genome (1.7% of all human genes),[14] many of which are pharmaceutically important because they regulate disease-related cellular processes.[15] The superfamily can be divided into three groups based on their activity. The first phosphorylates the alkyl hydroxyl of either serine or threonine residues,[16] the second modifies the phenolic hydroxyl of tyrosine residues,[17] and the third shows dual specificity for tyrosine and serine/threonine.[18] The sole three-dimensional structure of a protein kinase TSA complex is that formed between cAMP-dependent protein kinase A (PKA), ADP, a model target peptide (SP20), and an AlF_3^0 species.[19] This reported AlF_3^0 species is an isosteric but nonisoelectronic analogue of the transferring PO_3^- species, in apparent contrast to the charge balance observed in single-Mg^{2+} enzymes examined by ^{19}F NMR. While the structural features of the TSA complex have been interpreted[16] to support an in-line mechanism for phosphoryl transfer from ATP to the target serine, the charge imbalance from AlF_3^0 as compared to PO_3^- suggests that protein kinases have fundamentally different characteristics controlling phosphoryl transfer. To date, there are no equivalent structural data for a tyrosine kinase. As a result, sequence alignment (see Supporting Information) has been used to establish that active site residues coordinating to the transition state analogue in the PKA-ADP-AlF_3^0-SP20 complex are conserved throughout the superfamily, and so PKA has been necessarily used as a model in discussions of the activity of tyrosine kinases.[13]

To provide a direct analysis of the mechanistic relationship between protein kinases and single-Mg^{2+} enzymes, we have now applied ^{19}F NMR to the protein kinase MEK6[a]. MEK6 is a dual specificity kinase[18,20−22] that phosphorylates tyrosine-182 and threonine-180 of p38α MAP[b] kinase (p38α), which is thus activated.[20] This study provides a new entry to define detailed features of catalysis used by protein kinases, applicable to the phosphorylation of both serine/threonine and tyrosine residues.

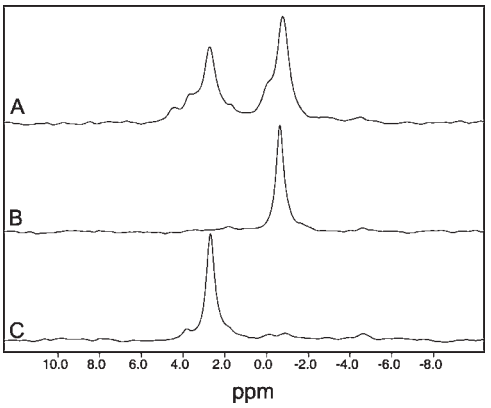

Figure 2. ^{31}P NMR spectra of p38α variants phosphorylated by MEK6dd: (A) p38α; (B) p38α(T180E); and (C) p38α(Y182E).

RESULTS

Phosphorylation of p38α by MEK6. In vivo, MEK6 requires activation through phosphorylation at serine-207 and threonine-211 before it can phosphorylate p38α. In this study, a constitutively active version[23] of MEK6 was used for simplicity. This double mutant, termed MEK6dd, has these two residues replaced by aspartates and retains high activity. To establish that the previously determined[21,22] specificity of MEK6dd for phosphorylation sites on p38α was maintained at the elevated protein concentrations required for NMR-based approaches, phosphorylation of p38α was monitored by ^{31}P NMR (Figure 2). The ^{31}P NMR spectrum of wild-type p38α after its biphosphorylation by MEK6dd shows two major resonances. The individual assignment of the resonances was achieved through the preparation of two mutant p38α proteins; independent substitutions of threonine-180 and tyrosine-182 by glutamate (termed T180E and Y182E, respectively) were introduced to remove one of the two phosphorylation sites (the carboxylate anion of the glutamate mimics the charge that would have been introduced by phosphorylation of p38α at that site). On treating the mutant p38α(T182E) with MEK6dd and ATP, a single phosphorus resonance appears at 3.8 ppm, corresponding to one of the two resonances observed for wild-type p38α. The equivalent experiment with p38α(Y180E) also generates a single resonance (at −0.4 ppm), corresponding to the second resonance observed for wild-type p38α. Hence, the downfield resonance is assigned to phosphothreonine-180, and the upfield resonance to phosphotyrosine-182, thus establishing that MEK6dd maintains specificity for these residues at elevated protein concentration. There is no evidence for nonspecific phosphorylation of p38α in the two mutant proteins.

Generation of an AlF_4^- Complex of MEK6. A solution of MEK6dd, p38α, ADP, $AlCl_3$ and NH_4F under the experimental conditions defined in Methods results in a ^{19}F NMR spectrum comprising four protein-bound resonances (see Figure 3 and Table 1). These resonances have intensities proportional to the

dx.doi.org/10.1021/ja1090035 |J. Am. Chem. Soc. 2011, 133, 3989–3994

concentration of MEK6dd and, by analogy to the spectra of TSA complexes of other phosphoryl transfer enzymes,[7−11] are assigned as the four fluorines of a protein-bound tetrafluoroaluminate ion (termed MEK6dd-ADP-AlF_4^--p38α TSA complex). The MEK6dd-ADP-AlF_4^--p38α TSA complex has a lifetime greater than 1 s, because presaturation of free F^- over this period had no effect on the TSA resonances. Comparison of the chemical shifts and linewidths of the four protein-associated resonances indicates significant differences in the nature of the protein moieties coordinating each fluoride. The fluoroaluminate species in such a complex is a six-coordinate, octahedral AlF_4^- moiety axially liganded by a β-oxygen from the ADP and a hydroxyl from the p38α substrate side chain (either threonine-180 or tyrosine-182; see Figure 1). No protein-bound metal fluoride complexes were detected in the absence of Al^{3+}, showing that the MEK6 active site does not support the formation of an MgF_3^- TSA complex. Moreover, neither TSA complex was formed with a peptide corresponding to the activation loop of p38α that contains threonine-180 and tyrosine-182 in the same sequence context.

Titration of a sample containing MEK6dd, p38α, ADP, and NH_4F with $AlCl_3$ shows a linear increase in the intensity of the fluoride peaks until the Al^{3+} is stoichiometric with the protein, after which point no further increase in intensity is observed (Figure 4). Therefore, the complex has a dissociation constant for Al^{3+} at least 50-fold lower than the MEK6dd concentration (240 μM), which is in the range observed for other metal fluoride TSA complexes.[24]

Inhibition of MEK6 by AlF_4^-. Evidence that the fluoroaluminate species behaves as a TSA is additionally provided by the inhibition of MEK6dd-mediated activation of p38α under the conditions of the NMR experiment. When p38α and MEK6dd are mixed in the presence of ATP (but not Al^{3+} and F^-), ADP production is only observed after a significant lag-time (Figure 5A), as detected using a continuous assay in which the generation of ADP is linked to NADH oxidation[25] and recorded using absorbance spectroscopy (see Methods). Many more ADP equivalents are produced than the number of phosphorylation sites in p38α that are available to MEK6dd (equivalent to 20 μM × 6220/M/cm = 0.12 A.U.). This is the result of the high ATP cleaving activity of activated p38α. The time-course of phosphorylation of p38α by MEK6dd was confirmed using a discontinuous Phos-Tag[26] SDS-PAGE-based assay (Figure 5B), and the increased rate of ADP production in the continuous

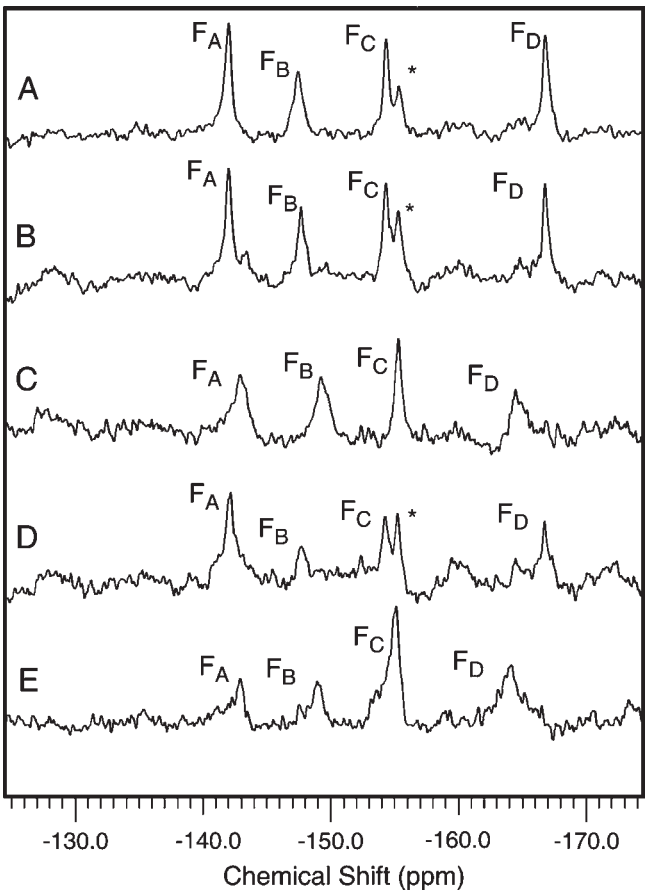

Figure 3. ^{19}F NMR spectra of TSA complexes between MEK6dd and p38α variants: (A) MEK6dd-ADP-AlF_4^--p38α; (B) MEK6dd-ADP-AlF_4^--p38α(T180A); (C) MEK6dd-ADP-AlF_4^--p38α(Y182F); (D) MEK6dd-ADP-AlF_4^--p38α(T180E); and (E) MEK6dd-ADP-AlF_4^--p38α(Y182E). The fluorine resonances are labeled A−D on the basis of their chemical shifts. *Residual resonance from free fluoroaluminate.

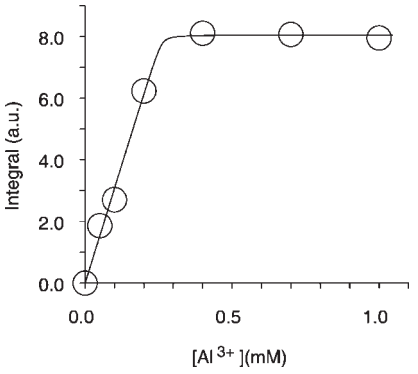

Figure 4. Intensity of the F_A resonance in ^{19}F NMR spectra of a solution containing MEK6dd, p38α, ADP, and NH_4F, on titration with $AlCl_3$. The MEK6dd concentration in these experiments was ∼240 μM. The theoretical curve is fitted for K_d = 400 nM, below which the value of chi squared does not reduce further.

Table 1. ^{19}F Chemical Shifts (ppm) in the MEK6 TSA Complexes

complex	F_A	F_B	F_C	F_D	free fluoroaluminate
MEK6dd-ADP-AlF_4^--p38α	−142	−148	−154	−167	−155
MEK6dd-ADP-AlF_4^--p38α(T180A)	−142	−148	−154	−167	−155
MEK6dd-ADP-AlF_4^--p38α(Y182F)	−143	−149	−155[a]	−164	−155[a]
MEK6dd-ADP-AlF_4^--p38α(T180E)	−142	−148	−154	−167	−155
MEK6dd-ADP-AlF_4^--p38α(Y182E)	−143	−149	−155[a]	−164	−155[a]

[a] Free fluoroaluminate and F_C are partly or completely overlapped.

dx.doi.org/10.1021/ja1090035 |J. Am. Chem. Soc. 2011, 133, 3989–3994

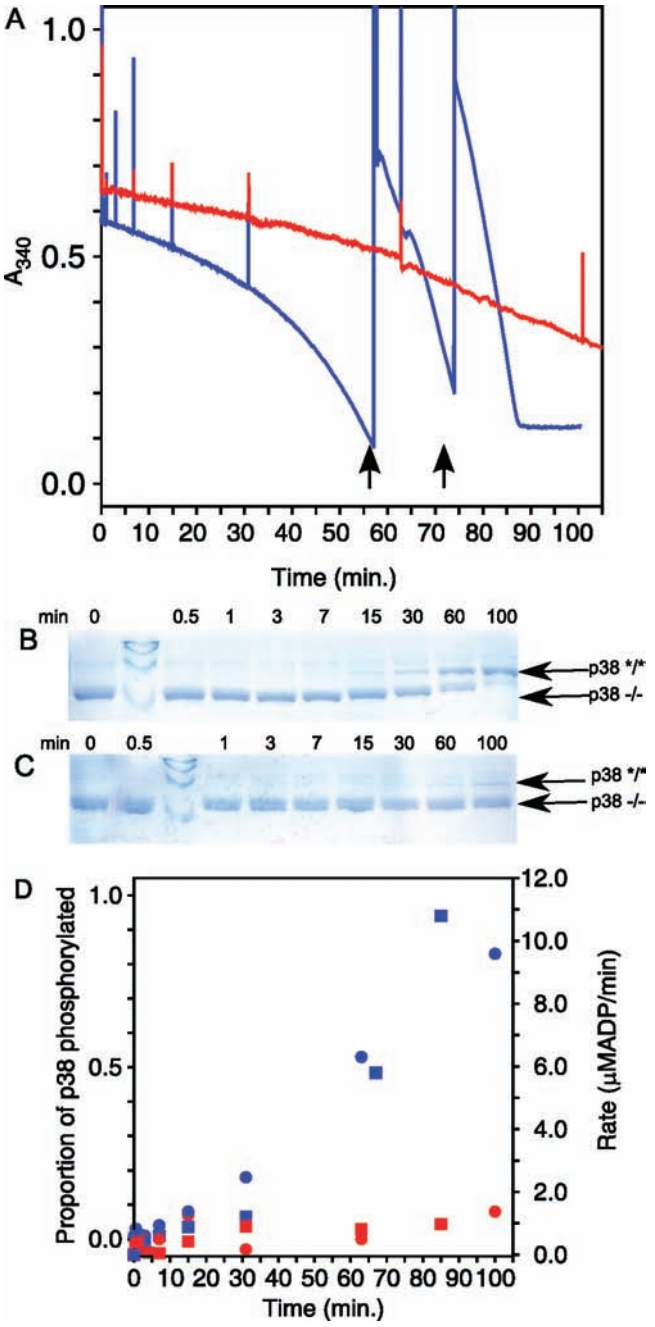

Figure 5. (A) PK/LDH linked continuous assay for ADP production by MEK6dd/p38α, in the absence (blue) and presence (red) of Al^{3+} and F^-. In the uninhibited reaction assay, additional aliquots of 100 μM NADH are added at 58 and 76 min; otherwise, this component would become limiting over the course of the assay. Other spikes in the data indicate where aliquots were taken for gel electrophoresis. (B and C) SDS-PAGE gels, supplemented with Phos-Tag, of the p38α assay mix quenched at the given times, (B) in the absence or (C) in the presence of Al^{3+} and F^-. (D) Relative intensities (●) of the Coomassie stained bands in (B) and (C) are compared to the instantaneous rates (■) of the reactions in (A) at the indicated time points. Blue and red symbols represent the absence and presence of Al^{3+} and F^-, respectively.

assay corresponds to the development of dually phosphorylated p38α (Figure 5D). Hence, the combination of continuous and discontinuous assays provides a reliable measure of MEK6dd activity. When this procedure is repeated in the presence of Al^{3+} and F^-, there is a substantial reduction in both ADP production (Figure 5A) and the formation of dually phosphorylated p38α (Figure 5C). Thus, the data in Figures 4 and 5 establish that the AlF_4^- species is a tight-binding inhibitor of MEK6.

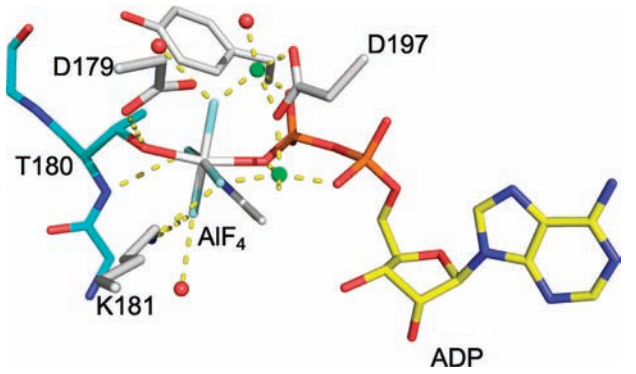

Figure 6. Homology model of the active site of MEK6 in an octahedral AlF_4^- TSA complex mimicking the phosphorylation of its substrate threonine residue (cyan cpk). The two catalytic Mg^{2+} ions are shown in green, the nucleotide is in yellow cpk, and MEK6 is in gray cpk.

Identification of Target Residues in the AlF_4^- Complexes. Two MEK6dd-ADP-AlF_4^--p38α TSA complexes might be formed, one with threonine-180 and one with tyrosine-182 in the position of the phosphoryl group acceptor. The fact that only four protein-bound ^{19}F resonances are observed for the MEK6dd-ADP-AlF_4^--p38α TSA complex (Figure 3A) indicates that one of the possibilities predominates. To identify which residue is preferred, two further mutant p38α proteins were generated, each having one of the phosphorylation sites modified to remove the relevant hydroxyl group. In one protein (T180A), threonine-180 is replaced by alanine, while in the other (Y182F), tyrosine-182 is replaced by phenylalanine. The ^{19}F NMR spectrum of the TSA complex formed with p38α(T180A) (Figure 3B, Table 1) is indistinguishable from the spectrum of the wild-type p38α TSA complex. By contrast, the TSA complex formed with p38α(Y182F) gives a significantly changed ^{19}F NMR spectrum (Figure 3C, Table 1). Relative to the positions in the wild-type p38α TSA complex, resonances corresponding to F_A, F_B, and F_C have shifted 1−2 ppm upfield, the resonance corresponding to F_D has shifted 2.8 ppm downfield, and the linewidths of these resonances are all much broader than those of the wild-type p38α TSA complex. (The resonance corresponding to F_C in the p38α(Y182F) TSA complex coincides with the residual peak from the free fluoroaluminate, but becomes resolved as a discrete signal at substoichiometric Al^{3+}.) These data establish that the wild-type p38α TSA complex with MEK6dd selects tyrosine-182 (rather than threonine-180) as the substrate ligand for the tetrafluoroaluminate moiety.

Data were also recorded for the T180E and Y182E mutant TSA complexes, which give ^{19}F NMR spectra (in terms of chemical shift) that are almost identical to those of the MEK6dd complexes formed with the T180A and Y182F mutants of p38α (Figure 3 B,C vs D,E). Therefore, the MEK6dd active site structure is not perturbed by the introduction of an anionic charge intended to mimic phosphorylation on the alternative amino acid residue.

Homology Modeling. The ^{19}F NMR properties of the various TSA complexes can be compared to a homology model of the MEK6dd-ADP-AlF_4^--p38α TSA complex based upon the PKA-

dx.doi.org/10.1021/ja1090035 |J. Am. Chem. Soc. 2011, 133, 3989–3994

Table 2. Deuterium Solvent-Induced Isotope Shifts (SIIS) of the MEK6 TSA Complexes[a]

SIIS/ppm	F_A	F_B	F_C	F_D
MEK6dd-ADP-AlF_4^--p38α(T180A)	1.1	0.7	0.4	0.2
MEK6dd-ADP-AlF_4^--p38α(Y182F)	1.1	1.0	0.3	0.1

[a] Uncertainties in SIIS are ±0.1 ppm.

ADP-AlF_3^0-SP20 complex (Figure 6). In this model, the AlF_4^- moiety is coordinated by residues lysine-181 (atom Nζ), asparagine-184 (atom Nδ2), alanine-63 (atom N), and the two catalytic Mg^{2+} ions, while aspartate-179 forms a regular hydrogen bond to the proton of the substrate hydroxyl group. The two most upfield fluorine resonances in the spectrum of the MEK6dd-ADP-AlF_4^--p38α TSA complex, F_C and F_D, have the narrowest linewidths, most upfield chemical shifts (Figure 3 and Table 1), and the lowest deuterium solvent-induced isotope shifts (SIIS; Table 2). This strongly indicates that each of them is coordinated by one of the two catalytic Mg^{2+} ions, which results in a reduced local proton density and higher intrinsic electron density[10] relative to the other two fluorides present, F_A and F_B. The small SIIS for F_D (≤0.2 ppm) resembles, for example, that of the F_C resonance in the equivalent TSA complex of β-phosphoglucomutase (βPGM) when the sugar is α-galactose 1-phosphate, and there is no coordinating hydrogen bond to F_C.[9] In contrast, the chemical shifts (Figure 3 and Table 1) and SIIS (Table 2) for F_A and F_B are typical of fluorides in other AlF_4^- TSA complexes coordinated only by hydrogen bonds.[8−11] Here, F_A has a SIIS of 1.13 ppm, which is, for example, closely similar to that of F_A in the TSA complex of β-PGM containing glucose 6-phosphate, where it is coordinated by three hydrogen bonds.[7] The close similarity of chemical shifts and SIISs in the tyrosine and threonine-based TSA complexes (Table 2) suggests that, while chemical shift differences respond to the nature of the two apical oxygen ligands, MEK6dd coordinates the transition state complex for both target amino acids in largely the same fashion.

DISCUSSION

Overall, these results establish conclusively the formation of tetrafluoroaluminate (AlF_4^-) moieties as the dominant species in aluminum fluoride TSA complexes mimicking the phosphorylation of p38α by MEK6. The data are fully consistent with a complex containing an octahedral AlF_4^- moiety in which two fluorines coordinate the two catalytic magnesium ions, the other two fluorines are hydrogen bonded to active site residues, and the aluminum is coordinated apically by ADP and by a side-chain oxygen from the substrate residue. With wild-type p38α there is a preference of at least 10-fold for formation of the complex with tyrosine-182. When tyrosine-182 is mutated to alanine or glutamate, the aluminum is then coordinated by the side-chain oxygen of threonine-180. Despite the differences in affinity, the electronic and protonic environments of the fluorides in the two TSA complexes are very similar. The observed preferential formation of the tyrosine TSA complex is in accord with biochemical experiments in a closely related system that show in vitro modification of the equivalent tyrosine precedes that of the threonine in the activation pathway.[27,28] Such priority for phosphorylation of tyrosine over threonine is likely to be determined by many contributing factors including, for example, the difference in nucleophilicity indicated by relative pK_a values for tyrosine and threonine. Moreover, the observed failure of MEK6 to form a TSA complex with a short peptide having the sequence of the target sites establishes the dominance of protein−protein interactions in achieving correct presentation of the target residue to the bound ATP. The hydrogen-bonding interaction of aspartate-179 with the substrate hydroxyl group is a clear indication of the existence of general acid−base catalysis in the phosphoryl transfer process.

The unit negative charge of the AlF_4^- species in the MEK6dd-ADP-AlF_4^--p38α TSA complexes is equivalent to that of the transferring PO_3^- group. This behavior of a phosphoryl transfer enzyme having two catalytic magnesium ions is in accord with the dominance of charge balance in the control of phosphoryl transfer in single magnesium enzymes,[8,11] and contrasts with the AlF_3^0 species reported in the crystal structure of the PKA-ADP-AlF_3^0-SP20 complex.[19] The MEK6 results thus demonstrate that the previously reported behavior of PKA is by no means general for protein kinases. It follows that the use of the PKA AlF_3^0 crystal structure as a basis for QM-MM computations of the behavior of other protein kinases[29] may have limitations if used for analysis of charge distribution in its transition state conformation. Overall, it is clear that the utilization of metal fluorides as the core of transition state analogues for phosphoryl transfer has clear potential to unravel the mechanistic complexities of protein kinases. In particular, the integration of multinuclear NMR data with protein crystallography and computational methods provides a powerful, symbiotic approach.

METHODS

Both MEK6dd and p38α (wild type/mutants) were expressed in Rosetta (DE3) pLysS *E. coli* cells grown in LB media as His_6-tagged proteins encoded by pET-BS(+) and pET-15b vectors, respectively. Expression was induced by addition of IPTG (1 mM final concentration) once cultures had reached an OD of 0.8. Cells were incubated for a further 3 h at 37 °C following induction. Purification of the protein from clarified cell lysate by Talon (Clontech) affinity chromatography (using 150 mM imidazole to elute the protein) was followed in the case of p38α by cleavage of the His-tag by thrombin. A final purification step through size exclusion chromatography yielded 15 mg L^{-1} MEK6dd, and a final purification step through ion exchange chromatography yielded 60 mg L^{-1} p38α. The p38α mutants T180A, T180E, Y180F, and Y180E were produced using the QuikChange procedure (Stratagene, U.S.). p38α samples used in enzyme assays were treated with 1 U λ-phosphatase (New England Biolabs) overnight at 4 °C, because of partial phosphorylation resulting from recombinant expression. The peptide corresponding to the activation loop of p38α has the sequence GLARHTDDEMTGYVAT and was obtained from Peptide Protein Research, UK.

The TSA complexes were generated by mixing 300 μM p38α with 250 μM MEK6dd, 5 mM ADP, 10 mM $MgCl_2$, 210 μM $AlCl_3$, and 10 mM NH_4F in the standard buffer of 50 mM HEPES, 150 mM NaCl, 5 mM DTT, 2 mM NaN_3, pH 6.8. ^{19}F NMR spectra are accumulations of 96k transients recorded at 298 K on a Bruker Avance 500 MHz spectrometer (operating at 470.31 MHz for ^{19}F) equipped with a 5 mm QXI probe and field gradients and processed using FELIX (Felix, San Diego, CA). The free F^- signal (at −119 ppm) was suppressed using presaturation, which led to the almost complete suppression of the free fluoroaluminate resonances (*) through exchange. Solvent-induced isotope shifts (SIIS) for ^{19}F resonances were measured by comparing spectra for samples in 10% and 100% D_2O buffer and defined as $\delta_{H2O} - \delta_{D2O}$.[10,30] Fluoride coordinating protons in the protein were exchanged with deuterons prior to recording spectra. Integration of peaks was performed using FELIX, with the phase adjustment and baseline correction optimized for the

chosen peak. ^{31}P NMR spectra were accumulations of 128k scans at 298 K on a Bruker Avance 500 MHz spectrometer equipped with a 5 mm multinuclear probe tuned to ^{31}P (202.5 MHz).

Enzyme assays were conducted at 18 °C in the same buffer conditions as the NMR experiments, except for the omission of $AlCl_3$ and NH_4F in the uninhibited reactions. ADP production was detected by linked assay[25] through pyruvate kinase (PK) and lactate dehydrogenase (LDH) (Sigma), 10 U in 1 mL of assay mix. Other components were 0.1 mM NADH and 10 mM phosphoenolpyruvate. After a stable absorbance reading was established at 340 nm, ATP was added to 1 mM, resulting in a small decrease in absorbance through a ~1% contamination of the ATP stock with ADP. Inclusion of $AlCl_3$ and NH_4F did not affect this decrease and therefore had no effect on the linking enzymes. Addition of p38α to 10 μM resulted in no significant change in absorbance after 2 min, whereas subsequent addition of MEK6dd to 0.2 μM initiated reaction. Prior to addition of MEK6dd, an aliquot was taken and quenched with SDS-PAGE loading buffer (50 mM Tris/HCl pH 6.8, 100 mM dithiothreitol, 2% SDS (w/v), 0.1% bromophenol blue (w/v), 10% glycerol (v/v)) supplemented with 2 M urea, heated to 65 °C for 10 min, and then placed on ice until the end of the assay. At various time points, further aliquots were taken and quenched in the same way.

The phosphorylation status of p38α in samples taken from the continuous assay was assessed by SDS-PAGE using gels prepared with 10% v/v acrylamide, 0.3% v/v bisacrylamide, 50 μM PhosTag (Wako Pure Chemical Industries, Ltd., Osaka, Japan)[26] and $MoCl_2$. Migration of protein bands was assigned by comparison with phosphatase-treated, untreated, and MEK6-activated p38α samples. Coomassie staining density was assessed from electronically scanned images of gels analyzed using ImageJ (NIH).

The model of the MEK6 active site based on the coordinates of the crystal structure of the PKA-ADP-AlF_3^0-SP20 complex (Protein Data Bank code 1l3r) was performed using Swiss Model in automated mode,[31] and then the AlF_4^- peptide and nucleotide placed in the active site by superposition. The resulting structure was then energy minimized using the OPLSAA forcefield[32] with TIP4P water[33] and PME electrostatics in the GROMACS environment.[34] Parameters for ADP were taken from Meagher et al.,[35] and AlF_4^- was derived from XPLOR restraints provided by the HIC-Up database.[36]

■ ASSOCIATED CONTENT

Supporting Information. Kinase sequence alignment. This material is available free of charge via the Internet at http://pubs.acs.org.

■ AUTHOR INFORMATION

Corresponding Author
m.j.cliff@shef.ac.uk; j.waltho@shef.ac.uk

■ ACKNOWLEDGMENT

We thank BBSRC and the China Scholarship Council for financial support (award NSFC 20732004), and Vertex Pharmaceuticals, Cambridge, MA, for p38α and MEK6 expression vectors.

■ REFERENCES

(1) Lad, C.; Williams, N. H.; Wolfenden, R. *Proc. Natl. Acad. Sci. U.S.A.* **2003**, *100*, 5607–5610. (a) MEK 6; MAP/ERK Kinase6. (b) MAP mitogen activated protein kinase.
(2) Bowler, M. W.; Cliff, M. J.; Waltho, J. P.; Blackburn, G. M. *New J. Chem.* **2010**, *34*, 784–794.
(3) Cleland, W. W.; Hengge, A. C. *Chem. Rev.* **2006**, *106*, 3252–3278.
(4) Wittinghofer, A. *Curr. Biol.* **1997**, *7*, R682–R685.
(5) Graham, D. L.; Lowe, P. N.; Grime, G. W.; Marsh, M.; Rittinger, K.; Smerdon, S. J.; Gamblin, S. J.; Eccleston, J. F. *Chem. Biol.* **2002**, *9*, 375–381.
(6) Messmore, J.; Raines, R. *J. Am. Chem. Soc.* **2000**, *122*, 9911–9916.
(7) Baxter, N. J.; Olguin, L. F.; Golicnik, M.; Feng, G.; Hounslow, A. M.; Bermel, W.; Blackburn, G. M.; Hollfelder, F.; Waltho, J. P.; Williams, N. H. *Proc. Natl. Acad. Sci. U.S.A.* **2006**, *103*, 14732–14727.
(8) Baxter, N. J.; Blackburn, G. M.; Marston, J. P.; Hounslow, A. M.; Cliff, M. J.; Bermel, W.; Williams, N. H.; Hollfelder, F.; Wemmer, D. E.; Waltho, J. P. *J. Am. Chem. Soc.* **2008**, *130*, 3952–3958.
(9) Baxter, N. J.; Hounslow, A. M.; Bowler, M. W.; Williams, N. H.; Blackburn, G. M.; Waltho, J. P. *J. Am. Chem. Soc.* **2009**, *131*, 16334–16335.
(10) Baxter, N. J.; Bowler, M. W.; Alizadeh, T.; Cliff, M. J.; Hounslow, A. M.; Wu, B.; Berkowitz, D. B.; Williams, N. H.; Blackburn, G. M.; Waltho, J. P. *Proc. Natl. Acad. Sci. U.S.A.* **2010**, *107*, 4555–4560.
(11) Cliff, M. J.; Bowler, M. W.; Varga, A.; Marston, J. P.; Szabo, J.; Hounslow, A. M.; Baxter, N. J.; Blackburn, G. M.; Vas, M.; Waltho, J. P. *J. Am. Chem. Soc.* **2010**, *132*, 6507–6516.
(12) Lee, J. Y.; Yang, W. *Cell* **2006**, *127*, 1349–1360.
(13) Huse, M.; Kuriyan, J. *Cell* **2002**, *109*, 275–282.
(14) Manning, G.; Whyte, D. B.; Martinez, R.; Hunter, T.; Sudarsanam, S. *Science* **2002**, *298*, 1912–1934.
(15) Pawson, T.; Scott, J. D. *Trends Biochem. Sci.* **2005**, *30*, 286–290.
(16) Fischer, E. H.; Krebs, E. G. *J. Biol. Chem.* **1955**, *216*, 121–132.
(17) Hunter, T. *Curr. Opin. Cell Biol.* **2009**, *21*, 140–146.
(18) Raingeaud, J.; Gupta, S.; Rogers, J. S.; Dickens, M.; Han, J.; Ulevitch, R. J.; Davis, R. J. *J. Biol. Chem.* **1995**, *270*, 7420–7426.
(19) Madhusudan; Akamine, P.; Xuong, N. H.; Taylor, S. S. *Nat. Struct. Biol.* **2002**, *9*, 273–277.
(20) Han, J.; Lee, J.; Jiang, Y.; Li, Z.; Feng, L.; Ulevitch, R. *J. Biol. Chem.* **1996**, *271*, 2886–2891.
(21) Raingeaud, J.; Whitmarsh, A. J.; Barrett, T.; Derijard, B.; Davis, R. J. *Mol. Cell. Biol.* **1996**, *16*, 1247–1255.
(22) Zhang, Y. Y.; Mei, Z. Q.; Wu, J. W.; Wang, Z. X. *J. Biol. Chem.* **2008**, *283*, 26591–601.
(23) Alonso, G.; Ambrosino, C.; Jones, M.; Nebreda, A. R. *J. Biol. Chem.* **2000**, *275*, 40641–40648.
(24) Golicnik, M.; Olguin, L. F.; Feng, G.; Baxter, N. J.; Waltho, J. P.; Williams, N. H.; Hollfelder, F. *J. Am. Chem. Soc.* **2009**, *131*, 1575–88.
(25) Anderson, K.; Murphy, A. *J. Biol. Chem.* **1983**, *258*, 14276–14278.
(26) Kinoshita, E.; Kinoshita-Kikuta, E.; Takiyama, K.; Koike, T. *Mol. Cell. Proteomics* **2006**, *5*, 749–757.
(27) Ferrell, J. E.; Bhatt, R. R. *J. Biol. Chem.* **1997**, *272*, 19008–19016.
(28) Askari, N.; Beenstock, J.; Livnah, O.; Engelberg, D. *Biochemistry* **2009**, *48*, 2497–2504.
(29) Turjanski, A. G.; Hummer, G.; Gutkind, J. S. *J. Am. Chem. Soc.* **2009**, *131*, 6141–6148.
(30) Hagen, D. S.; Weiner, J. H.; Sykes, B. D. *Biochemistry* **1979**, *18*, 2007–2012.
(31) Arnold, K.; Bordoli, L.; Kopp, J.; Schwede, T. *Bioinformatics* **2006**, *22*, 195–201.
(32) Jorgensen, W. L.; Maxwell, D. S.; Tirado-Rives, J. *J. Am. Chem. Soc.* **1996**, *118*, 11225–11236.
(33) Jorgensen, W. L.; Chandrasekhar, J.; Madura, J. D.; Impey, R. W.; Klein, M. L. *J. Chem. Phys.* **1983**, *79*, 926–935.
(34) Hess, B.; Kutzner, C.; van der Spoel, D.; Lindahl, E. *J. Chem. Theory Comput.* **2008**, *4*, 435–447.
(35) Meagher, K. L.; Redman, L. T.; Carlson, H. A. *J. Comput. Chem.* **2003**, *24*, 1016–1025.
(36) Kleywegt, G.; Jones, T. *Acta Crystallogr., Sect. D* **1998**, *54*, 1119–1131.